Metabolic Engineering Communications 14 (2022) e00193

Contents lists available at ScienceDirect

Metabolic Engineering Communications

journal homepage: www.elsevier.com/locate/mec

Thermodynamics contributes to high limonene productivity in cyanobacteria

Shrameeta Shinde [a], Sonali Singapuri [a], Zhenxiong Jiang [a], Bin Long [b], Danielle Wilcox [a], Camille Klatt [a], J. Andrew Jones [c], Joshua S. Yuan [b], Xin Wang [a,*]

[a] Department of Microbiology, Miami University, Oxford, OH, 45056, USA
[b] Synthetic and Systems Biology Innovation Hub, Department of Plant Pathology and Microbiology, Texas A&M University, College Station, TX, 77843, USA
[c] Department of Chemical, Paper, and Biomedical Engineering, Miami University, Oxford, OH, 45056, USA

ARTICLE INFO

Keywords:
Cyanobacteria
Thermodynamics
Terpene biosynthesis
Limonene
Sigma factor

ABSTRACT

Terpenoids are a large group of secondary metabolites with broad industrial applications. Engineering cyanobacteria is an attractive route for the sustainable production of commodity terpenoids. Currently, a major obstacle lies in the low productivity attained in engineered cyanobacterial strains. Traditional metabolic engineering to improve pathway kinetics has led to limited success in enhancing terpenoid productivity. In this study, we reveal thermodynamics as the main determinant for high limonene productivity in cyanobacteria. Through overexpressing the primary sigma factor, a higher photosynthetic rate was achieved in an engineered strain of *Synechococcus elongatus* PCC 7942. Computational modeling and wet lab analyses showed an increased flux toward both native carbon sink glycogen synthesis and the non-native limonene synthesis from photosynthate output. On the other hand, comparative proteomics showed decreased expression of terpene pathway enzymes, revealing their limited role in determining terpene flux. Lastly, growth optimization by enhancing photosynthesis has led to a limonene titer of 19 mg/L in 7 days with a maximum productivity of 4.3 mg/L/day. This study highlights the importance of enhancing photosynthesis and substrate input for the high productivity of secondary metabolic pathways, providing a new strategy for future terpenoid engineering in phototrophs.

1. Introduction

Terpenoids are a large class of secondary metabolites produced in all living organisms. Characterized by their extensive structural diversity, many terpenoids are of significant interest to humans because of their applications as advanced biofuels, pharmaceuticals, and nutraceuticals (Ajikumar et al., 2008; Wang et al., 2015). Photosynthetic terpene production is an attractive route because of its carbon-neutral property. Cyanobacteria fix carbon dioxide by harnessing solar energy and directly convert it into various metabolites, making them promising biocatalysts for chemical production (Knoot et al., 2018).

Engineering terpene pathways in cyanobacteria commenced with a pioneering work of isoprene (C_5) production (Lindberg et al., 2010), followed by the photosynthetic production of longer chain terpenoids including limonene, bisabolene, phellandrene, manoyl oxide, and squalene (Davies et al., 2014; Englund et al., 2014, 2015; Formighieri and Melis, 2014). Limonene, a monoterpene (C10), is commercially used in the fragrance industry but recently has gained more attention due to its potential as drop-in biofuels (Chuck and Donnelly, 2014). Several follow-up studies focused on engineering the methylerythritol 4-phosphate (MEP) pathway to improve terpene titers (Choi et al., 2016; Englund et al., 2015; Halfmann et al., 2014; Kiyota et al., 2014). With the exception of one study where a high isoprene flux was achieved in cyanobacteria (Gao et al., 2016), all other studies showed only marginal increases in terpene titers (Formighieri and Melis, 2016). These studies demonstrated the possibility to produce terpenes in phototrophs but all were limited by low productivities for a scalable photosynthetic microbial production platform (Lin and Pakrasi, 2019). To attain high product titers, a few recent studies have attempted alternative strategies to boost terpene production in cyanobacteria. Guided by computational modeling, engineering the pentose phosphate pathway achieved a limonene titer of 6.7 mg/L in *Synechocystis* sp. PCC 6803 (Lin et al., 2017). In another study, a fast-growing cyanobacterium *Synechococcus elongatus* UTEX 2937 was genetically modified to attain the limonene titer of 16.4 mg/L during a 2-day production period (Lin et al., 2021). Despite these efforts, the traditional pathway engineering showed

* Corresponding author.
E-mail address: xwang@miamioh.edu (X. Wang).

https://doi.org/10.1016/j.mec.2022.e00193
Received 3 October 2021; Received in revised form 18 January 2022; Accepted 19 January 2022
Available online 22 January 2022

limited success in enhancing the MEP-derived terpene flux in cyanobacteria.

A major limitation in achieving high terpene yields through the MEP pathway is low carbon partitioning (Melis, 2013). Both thermodynamics and enzyme kinetics contribute to increasing carbon flux toward target pathways (Noor et al., 2014, 2016; Wu et al., 2020). However, secondary metabolism such as the MEP pathway has evolved with enzymes of low efficiency (Bar-Even et al., 2011), limiting its "pull" capacity to enhance carbon flux. We argue that enhancing the MEP pathway flux requires a strong "push" effect in the first place, i.e. a strong thermodynamic driving force determined by substrate input. However, terpene production in cyanobacteria is constrained by thermodynamics due to limited CO_2 delivery to cells. Therefore, enhancing carbon fixation could improve the thermodynamic landscape, resulting in a productive pathway for synthesizing secondary metabolites. Engineering primary transcription factors can improve photosynthetic efficiency, potentially leading to overall increased carbon fixation and improved substrate input to target pathways. However, only a few studies reported transcription factor engineering to improve chemical production in cyanobacteria (Kaczmarzyk et al., 2014; Osanai et al., 2013). Here in this study, we implement this strategy in a highly efficient limonene-producing *Synechococcus elongatus* PCC 7942 strain L1118 (hereafter *Synechococcus* L1118) from our previous study (Wang et al., 2016), to further improve limonene production. We show that sigma factor overexpression leads to enhanced photosynthesis in *S. elongatus*, improving the "source" capacity for efficient limonene production.

2. Materials and methods

2.1. Bacterial strains and growth conditions

All recombinant plasmids were assembled and transformed in *Escherichia coli* DH5α strains that were routinely maintained on LB medium with respective antibiotics. Seed cultures for *Synechococcus elongatus* PCC 7942 strains were typically grown under 20 μmol photons $m^{-2}{\cdot}s^{-1}$ at 30 °C using BG11 growth medium supplemented with 10 mM N-[Tris(hydroxymethyl)methyl]-2-aminoethanesulfonic acid (TES, pH 7.8) and 20 mM bicarbonate ($NaHCO_3$). For limonene productivity, cells were grown continuously in 1-L Roux bottles containing 500 mL of BG11 supplemented with 10 mM TES and 20 mM $NaHCO_3$ aerated with ambient air under 50 μmol photons under $m^{-2}{\cdot}s^{-1}$ illumination from cool white fluorescent light tubes for five days unless specified otherwise. Initial growth experiments of engineered strains were performed in the Multi-Cultivator (Photon Systems Instruments, Czech Republic) at 50 μmol photons under $m^{-2}{\cdot}s^{-1}$ illumination with growth recorded as optical density (OD) 720 nm readings every 10 min. The engineered strains were grown in antibiotics with a final concentration of 2 mg/L spectinomycin/streptomycin (a neutral site I targets) and/or 5 mg/L kanamycin (a neutral site II target) as per the strain requirement. The stocks for cyanobacterial strains were maintained on BG11 solid media plates. All strains and plasmids used in this study are listed in Table S1.

2.2. Plasmid construction

Overexpression plasmids for all sigma factor (SF) genes and *bicA* started with PCR amplification of the Km selective marker gene, DNA segments encoding nine SFs, and BicA from the genome of *Synechococcus elongatus* PCC 7942 and *Synechocystis* sp. PCC 6803, respectively using Phusion polymerase (New England Biolabs, MA, USA). The purified DNA fragments were assembled with the backbone of pAM1579 (neutral site II) using the HiFi DNA Assembly master mix (New England Biolabs, MA, USA). All overexpression plasmids targeting the neutral site II of the *S. elongatus* genome in this study (Table S1) have LacO promoter but lack the LacI repressor coding DNA segment thus enabling constitutive expression of respective SF gene. Plasmid to express the limonene synthase (LS) gene at the neutral site I in *S. elongatus* was designed in our previous study (Wang et al., 2016).

2.3. Transformation of engineered strains

Transformation of *S. elongatus* strains was accomplished following the protocol described previously (Golden et al., 1987). Briefly, one mL of the wild-type *S. elongatus* strain was taken from logarithmic phase culture grown in BG11 medium with OD_{730} approximately 0.7–0.8. Next, cells were pelleted by centrifugation and resuspended in 1 mL of 10 mM sodium chloride. After centrifugation, the pellet was resuspended in 200 μL of fresh BG11 medium and mixed with 100 ng DNA of plasmid. The samples are mixed properly via pipette and were incubated in dark for about 5 h at 30 °C, with constant shaking at a low-speed rotator. Cells were then spread onto BG11 plates supplemented with appropriate selective antibiotics and incubated under 20 μmol photons $m^{-2}{\cdot}s^{-1}$ light at 30 °C for 5–7 days to obtain transformants. *S. elongatus* contains multiple (3–6) genome copies in a cell (Rubin et al., 2015) and thus segregation PCR was performed to obtain a clean mutant.

2.4. Limonene quantification by gas chromatography – mass spectrometry (GC-MS)

Limonene from the engineered *S. elongatus* strains L*rpoD*, L*bicA*, and L1118 (control) was collected using an absorbent trap containing HayeSep porous polymers (Sigma, USA) attached to the outlet of individual 1-L Roux bottles. Every day, limonene was eluted from the trap with 1 mL hexane supplemented with 10 μg/mL cedrene (Sigma, USA) as the internal standard. One μL of the eluted sample was analyzed by GC-MS in a Thermo Trace 1300 ISQ quadrupole (QD) (Thermo Fisher Scientific, USA) system. The samples were injected into a Zebron GC column (ZB-5MSplus, 30 m × 0.25 mm x 0.25 μm). The GC program was set for an initial hold at 40 °C for 3 min, followed by temperature increase to 140 °C at the rate of 20 °C/minute and then to a final temperature of 300 °C at the increment of 25 °C/minute. Limonene concentration was calculated based on an established standard curve with known limonene concentrations. The final limonene yield was adjusted by the trap recovery rate, determined by supplementing 500 mL of BG11 with various concentrations of limonene (Fig. S1). Limonene was collected the next day using the procedure described above, and a standard curve was generated to calculate the limonene recovery. The average limonene productivity for strain comparisons was calculated from the log-phase cells during a 3-day limonene production period.

2.5. Shotgun proteomics

Synechococcus L1118 and L*rpoD* were grown to log phase in 1 L Roux culture bottles as described above. Ten mL of cells with the OD_{730} of about 1.0 were collected in triplicates and centrifuged at 7200 g for 20 min at 4 °C. Briefly, the sample preparation involves resuspension of cell pellets in 1 mL Lysis buffer (50 mM Tris-HCl, 0.1% [w/v] n-dodecyl b-D-maltoside, and 1X Halt™ protease and phosphatase inhibitor cocktail (Thermo Fisher Scientific, Rockford, IL, USA) followed by homogenous cellular lysis with six cycles of 10 s at 2400 rpm using a bead-beater. Samples were centrifuged at 13,000 g and 4 °C for 30 min to collect protein extract in the supernatant. Bradford assay (Thermo Fisher Scientific, USA) was performed to determine the protein concentration.

For each sample, 100 μg of total protein was treated with 8 M urea and 5 mM dithiothreitol (DTT) at 37 °C for 1 h, followed by incubation with 15 mM iodoacetic acid (IAA) at room temperature (RT) for 30 min. The protein sample was then diluted using Tris HCl buffer (50 mM Tris-HCl, 10 mM $CaCl_2$, pH 7.6) to attain the final urea concentration of 2 M. The diluted protein sample was subjected to enzymatic digestion using Trypsin Gold (Promega, USA) with a 1:100 (w/w) of trypsin to protein ratio at 37 °C for 20 h. The digested peptides were cleaned up using a Sep-Pak C18 column (Waters, USA) followed by peptide fractionation using the Pierce High pH Reverse-Phase Peptide Fractionation Kit

(Thermo Fisher Scientific, USA). Eight fractions of peptides from each sample were subjected to liquid chromatography-tandem mass spectrometry (MS/MS) analysis in a Thermo LTQ Orbitrap XL mass spectrometer (Thermo Fisher Scientific, USA). The data-dependent mode was used to operate the mass spectrometer along with scanning the mass range of 350 to 1800 mass-to-charge ratio at a resolution of 30,000. The 12 most abundant peaks were chosen and subjected to MS/MS analysis by collision-induced dissociation fragmentation. Raw data collected from MS/MS analysis was analyzed using the PatternLab for Proteomics program (version 4.1.0.17; Carvalho et al., 2016). The normalized spectral abundance factor (NSAF) was used to compare protein abundance in different groups (Zybailov et al., 2006). The proteomics data have been deposited to the ProteomeXchange Consortium via the PRIDE (Perez-Riverol et al., 2019) partner repository with the dataset identifier PXD028410.

2.6. Full absorbance spectra for engineered S. elongatus strains

Whole-cell absorbance wavelength scans were performed for *Synechococcus* L1118 and L*rpoD*, growing in BG11 supplemented with 20 mM $NaHCO_3$ under continuous light of 50 μmol photons $m^{-2}{\cdot}s^{-1}$ at 30 °C. For the assay, 200 μl of cells were used to measure the absorbance for a spectrum ranging from 300 nm to 700 nm with data points collected every 10 nm using a SpectraMax iD5 microplate reader (Molecular Devices). The absorbance scans were normalized by cell density (OD_{730}). All measurements were determined by averaging triplicates of independent cultures.

2.7. Oxygen evolution measurements

Two mL of limonene-producing cells, *Synechococcus* L1118 and L*rpoD*, from biological triplicates were used each day for photosynthesis activity measurement. Whole-cell oxygen evolution was measured during a 9-min window at room temperature with saturation light illumination in a Clark-type oxygen electrode (Qubit systems, Ontario, CN). No additional bicarbonate was supplemented in the electrode chamber as the growth medium contained 20 mM $NaHCO_3$. The data was analyzed using Logger Pro software supplied with the instrument. The collected cells were pelleted and used for chlorophyll estimation using a previously described protocol (Zavřel et al., 2015). The final oxygen evolution rate was corrected with the dark respiration rate and normalized to chlorophyll content.

2.8. Determination of dry cell weight (DCW)

The cell dry biomass weight was determined by following a previously published protocol (Broddrick et al., 2016). Briefly, 10 mL of *Synechococcus* L1118 and L*rpoD* cells growing at 30 °C and 50 μmol s^{-1} m^{-2} continuous light was collected by filtering through a pre-weighed 0.45-μm hydrophilic polypropylene filter (25-mm). Following filtration, the filters containing cells were dried at 90 °C for 1 h and weighed again after cooling to room temperature to determine the dry cell weight. Filters were further dried for additional time and weighed again to ensure complete drying. The correlation between OD and DCW was determined by plotting DCW against OD_{730} measured in the range of 0.03–1.0.

2.9. Determination of glycogen content

Five mL of cells from the exponential growth phase cultures of *Synechococcus* L1118, L*rpoD*, and L*bicA* were collected, centrifuged at 6000 g and 4 °C for 10 min, and washed with 1 mL of 50 mM Tris-HCl buffer, pH 8.0 twice with a final resuspension in 500 μL of Tris-HCl buffer. All samples henceforth were maintained on ice. The resuspended cells were lysed with bead beating cycles of 10 s on and 2 min off on ice at 2400 rpm for a total of twelve cycles. The cell lysate was collected by centrifugation at 6000*g* and 4 °C for 10 min and used for protein estimation by Bradford assay (Thermo Fisher Scientific, USA). The values were used to normalize the glycogen content on a protein content basis. Following protein estimation, glycogen in 100 μL of the lysate was precipitated following a previously described protocol (De Porcellinis et al., 2017). Briefly, the samples were treated with 900 μL of 96% (v/v) ethanol in 2 mL screw-cap test tubes, heated at 90 °C for 10 min, and incubated on ice for 30 min to remove chlorophyll. Samples were then centrifuged at 20,000 g and 4 °C for 30 min to obtain the pellet containing glycogen. The pellet was air-dried for 5 min at room temperature, solubilized in 100 μL of 50 mM sodium acetate (pH 5), and hydrolyzed to glucose by the addition of 50 μL of 8 U/mL amyloglucosidase and 2 U/mL α-amylase, respectively. The mixture was vortexed vigorously to ensure proper solubilization and heated at 60 °C on a heating block for 2 h. The samples were centrifuged at 10,000×*g* for 5 min and the supernatant was used to estimate the glucose concentration using Glucose oxidase peroxidase (GOD-POD) reagent (Megazyme, USA) in a 96-well plate assay format. Specifically, 100 μL of the supernatant was mixed with 150 μL of GOD-POD while 100 μL of 50 mM sodium acetate (pH 5) was used to serve as a negative control. The plate was incubated at 25 °C for 30 min and absorbance was recorded at 510 nm using SpectraMax iD5 microplate reader (Molecular Devices). The glucose concentration in the samples was estimated using a calibration curve obtained from the glucose standards made in 50 mM sodium acetate (pH 5). Glycogen measurements were normalized to dry cell weight (DCW) based on the OD-DCW standard curve of the L1118 strain determined above.

2.10. Intracellular sucrose measurements

The cells for *Synechococcus* L1118, L*rpoD*, and L*bicA* strains were collected from cultures growing at 30 °C and 50 μmol s^{-1} m^{-2} continuous light every 24 h for five days and stored in −20 °C. Samples were used to perform sucrose assays in 96-well plate format. In the assay plates, 50 μL of culture was mixed with 25 μL of lysis solution (2% DTAB in 0.4 M NaOH) followed by 10 min incubation at room temperature. Following the lysis of the cells, 25 μL of 0.4 M HCl was added to neutralize the solution. One set of technical replicates served as a negative control by addition of 50 μL of sodium acetate buffer while another set of technical replicates was used for sucrose hydrolysis by addition of 50 μL premixed invertase solution (45 μL of sodium acetate buffer and 5 μL of 8 U/mL invertase). The assay plate was incubated for 45 min at 50 °C in the dark. Next, 100 μL of GOPOD reagent (Megazyme, USA) was added to each well, the plate was incubated at 50 °C for 20 min and the absorbance was read at 510 nm using SpectraMax iD5 microplate reader (Molecular Devices). Sucrose content was normalized to dry cell weight (DCW) based on the OD-DCW standard curve of the L1118 strain determined above.

2.11. Flux balance analysis

The previously constructed genome-scale model (GEM) *i*JB785 (Broddrick et al., 2016) was adopted for the simulation of the metabolic network in our study. A new reaction by limonene synthase was added to *i*JB785 to construct our model. All constraints of the model *i*JB785 were kept in the new model, including flux constraint of enzymes (transhydrogenase, ornithine transaminase, cytochrome oxidase, and lactate dehydrogenase), oxygen evolution constraint, maximum PSII flux constraint, and metabolite channeling constraint of phosphoketolase pathway. The objective function was set to maximize the biomass. The biomass components in model *i*JB785 were slightly adjusted by adding limonene as an additional component with its weight coefficient estimated based on the measured limonene flux in this work. Flux balance analysis was run using the settings where the irradiance was 30 μmol s^{-1} m^{-2} (Low light, LL) and 50 μmol s^{-1} m^{-2} (High light, HL) respectively. The fluxes of all reactions throughout 240 time points were recorded

into a matrix and saved in separate files for further data analysis. The first column of the matrix which represents the fluxes of the outermost layer of cultures in the flask at time point 0 was selected for the flux comparison between two conditions. Fluxes under both LL and HL conditions, as well as their flux ratio, were visualized using Escher. In addition, Flux Variability Analysis (FVA) for maximum growth was conducted to reveal the flux boundaries of reaction steps related to photosynthesis.

2.12. Growth optimization for limonene production

Cultures of *Synechococcus* L1118 and L*rpoD* (50 mL) were grown in triplicates in Multi-Cultivator MC 1000-OD (Qubit systems, Ontario, CN) connected to DASGIP gas mixing module MX4/4 (DASGIP, Jülich, Germany). Throughout the experiment, cultures were cultivated in a CD medium, prepared as described in (Rodrigues and Lindberg, 2021) aerated with 5% CO_2 with a constant flow rate of 2.5 L/h at 37 °C with incremental light illumination. Specifically, an initial OD_{730} of 0.45 cells were used as the starting culture and grown with the light illumination of 250 μmol s^{-1} m^{-2} and 500 μmol s^{-1} m^{-2} on day 1 and day 2, followed by an increased light intensity to 1000 μmol s^{-1} m^{-2} and 1400 μmol s^{-1} m^{-2} on day 3 and day 4 respectively. Cultures were grown at the maximal light (1400 μmol s^{-1} m^{-2}) for the remaining duration of the experiment. Growth and limonene production were monitored as procedures described in the above section.

3. Results and discussion

3.1. Overexpression of essential sigma factors enhances limonene production in S. elongatus

Limonene is a non-native monoterpene for *Synechococcus elongatus* PCC 7942 (hereafter *S. elongatus*). To determine the influence of sigma factors (SF) on limonene production, nine known sigma factors from *S. elongatus* (Table S2) were individually inserted into the neutral site II of *Synechococcus* L1118 genome under the control of the P*lac* promoter. The transformants were confirmed by segregation PCR for insertion of SF and limonene synthase (LS) genes at the neutral site II and I, respectively. The growth of all SF strains was monitored by absorbance at 720 nm in comparison to the strain *Synechococcus* L1118. These SFs showed a varied effect on cell growth. Specifically, overexpression of genes encoding RpoD, RpoE, SigD, and SigA had minimal impact on cell growth whereas SigB, SigC, SigF1, SigF2, and SigI lowered cell growth considerably (Fig. 1A and B). The observed growth behaviors agree with the roles of these SFs in *S. elongatus*. RpoD is the sole essential SF that regulates the expression of housekeeping genes (Imamura et al., 2003). A homolog of RpoE (SigG) in *Synechocystis* sp. PCC 6803 was identified to be important for cellular growth as knockout mutants exhibited decreased growth (Huckauf et al., 2000). SigD is known to cause light-induced expression of photosynthetic genes encoding proteins associated with phycocyanin, cytochrome *b*6, PSII, and PSI complexes (Yoshimura et al., 2007). RpoD, RpoE, and SigD are SFs that could potentially benefit cell growth when a threshold level of expression is reached. The observed minimal impact on cell growth is thus likely due to their expression levels not being high enough to support faster growth in the engineered strains.

Sig A, B, C, and F2 form a sigma factor cascade to modulate the complex circadian gene network depending on environmental cues (Fleming and O'Shea, 2018). Any perturbations in the levels of these SFs can potentially alter the metabolism and growth of cyanobacteria. However, the exact role of SigA is still elusive, thus hard to pinpoint its effect on cell growth. SigB, on other hand, is a stress-responsive SF triggered by stressors like high light and high salt (Kanesaki et al., 2002; Tuominen et al., 2003). When growing under high light and salt conditions, a *Synechocystis* sp. PCC 6803 mutant containing only the SigB from the non-essential group 2 SFs showed downregulated expression of genes related to chlorophyll and phycobilin synthesis while upregulating expression of genes involved in carotenoids and flavodiiron proteins

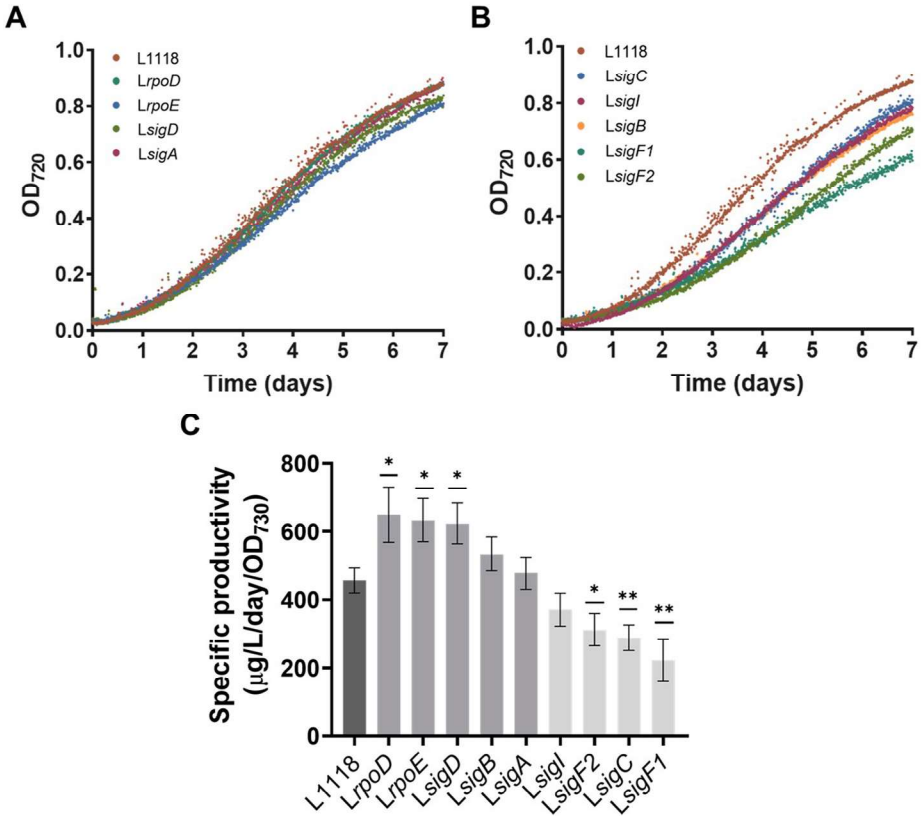

Fig. 1. Impact of sigma factor overexpression on *S. elongatus* growth and limonene production under continuous light. A and B: Growth profile of sigma factor overexpression strains along with *Synechococcus* L1118 strain as a control. The study involves individual overexpression of endogenous SF genes. Each strain was tested with four biological replicates. C: Specific productivity of limonene in all nine *Synechococcus* sigma factor overexpression strains relative to the L1118 strain. All strains were grown under continuous 50 μmol photons $m^{-2}{\cdot}s^{-1}$ light at 30 °C with 20 mM bicarbonate as the substrate for 7 days. Error bars indicate the SD; two-tailed Student's t-tests were used to compare specific productivity of limonene *, $P < 0.05$ and **, $P < 0.005$.

(FDPs) synthesis (Hakkila et al., 2013). Carotenoids and FDPs are involved in photoprotective mechanisms in cyanobacteria (Bersanini et al., 2014; Masojídek et al., 2013). Thus, overexpression of *sigB* in *S. elongatus* likely triggered a stress-response behavior, lowering photosynthesis and leading to slower growth as observed here. In *S. elongatus*, SigC is a negative regulator of *psbA1*, encoding one form of the photosystem II (PSII) core protein D1 (Martins et al., 2016). Overexpression of *sigC* is thus likely to downregulate photosynthesis, leading to slower growth as shown here (Fig. 1B). The negative impact on growth caused by SigF2 overexpression is likely caused by a disrupted sigma factor cascade network (Srivastava et al., 2021), leading to slower growth mimicking a stress response phenotype in *S. elongatus* (Fig. 1B).

Limonene production was also affected by SF overexpression. Specifically, overexpression of *rpoD*, *rpoE,* and *sigD* resulted in statistically higher specific limonene productivity, showing an approximate 1.7-, 1.6-, and 1.5-fold increases than the *Synechococcus* L1118 strain, respectively. On the other hand, overexpression of *sigB* and *sigA* increased limonene production moderately whereas *sigF1*, *sigI*, *sigF2,* and *sigC* considerably decreased the production levels (Fig.1C and Fig. S1A). These data highlight a trend that higher limonene yield is observed in SF engineered strains that had no or minimal changes in growth when compared to *Synechococcus* L1118. The only exception to this is the SigB overexpression strain with moderately increased limonene and significantly slower growth. Being a stress-responsive SF, a higher abundance of SigB most likely increased the production of carotenoids, a terpenoid molecule, via the MEP pathway. Limonene synthesis thus could have benefited from the increased MEP flux in the SigB overexpression strain. Higher limonene production in this study also aligns with sigma factor engineering in *Synechocystis* sp. PCC 6803 to enhance target compound yields. For example, one study overexpressed the SigE gene to accumulate polyhydroxybutyrate (PHB) as SigE is known to control sugar metabolism and increase the abundance of PHB precursor acetyl-CoA (Osanai et al., 2013).

3.2. Higher photosynthetic efficiency supports increased limonene production

Engineering essential sigma factors leads to improved limonene biosynthesis in *S. elongatus.* To understand how SF overexpression supports higher limonene productivity, we focused on one of the high-limonene producers, the strain *Synechococcus* L*rpoD*, for a comparative proteomics study. The RpoD abundance in the L*rpoD* strain was approximately 1.7-fold of the L1118 strain (Fig. S2A), confirming the successful overexpression of RpoD. Furthermore, both L1118 and L*rpoD* strains had similar LS levels that are in the top ten most abundant proteins in their proteome, suggesting that the limonene increase was not from increased LS expression in the L*rpoD* strain (Fig. S2B). On the other hand, many proteins belonging to the photosynthesis process are highly abundant in the L*rpoD* strain (Fig. 2 and S2C). Phycobilisomes (PBSs) are highly organized structures made of core and radical rods for light-harvesting in cyanobacteria (Zhao et al., 2017). The PBS core consists of pigmented allophycocyanin (APC) proteins (Apc A, B, D, and F) to which chromophores get attached and non-pigmented proteins (ApcC and ApcE) that hold the APC structure together and anchor it to the thylakoid membrane. All APC subunit proteins and PBS rod proteins (CpcA1, B1, C1, C2, D, and G) are highly abundant in the L*rpoD* strain with significant differences observed in ApcB, ApcC, CpcA1, CpcC2, and CpcG (Fig. 2A). Additionally, proteins involved in PBS degradation (CpcE, S, and NblB) (Zhao et al., 2017) were either not detected or had decreased abundance in the L*rpoD* strain (Fig, 2A). This indicates that the L*rpoD* strain potentially had increased light absorption to fulfill higher energy requirements. To confirm this, we measured the full light absorbance spectra of both L1118 and L*rpoD* cells consecutively for 4 days at 24-h intervals. The L*rpoD* cells showed a steady and significant increase in phycobilin and carotenoid levels with unaltered chlorophyll levels each day (Fig. 2B and S3), corroborating with proteomics results of higher PBS proteins in L*rpoD* and supporting our conclusion of higher energy absorption in the L*rpoD* strain.

In the reaction center, some of the PSII proteins were found more abundant in the L*rpoD* strain (Fig. S2C). The L*rpoD* cells have a higher abundance of accessory proteins Psb27, PsbU, and PsbN. The most significant difference in abundance was observed for PsbU protein (Fig. 2A). Multiple studies have highlighted the diverse roles of PsbU in cyanobacteria. Lack of PsbU decreases oxygen evolution capacity (Shen et al., 1997), making cells prone to photodamage (Balint et al., 2006) and affecting the coupling of PBSs to PSII complex (Veerman et al., 2005). A study in *S. elongatus* showed that lack of PsbU affected the electron transport in the PSII complex and potentially led to light

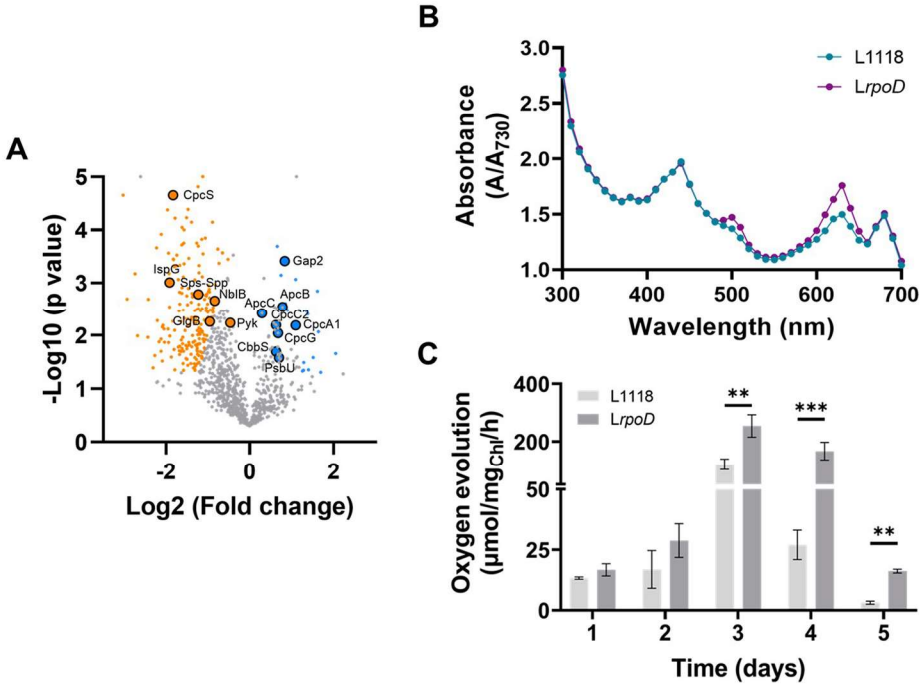

Fig. 2. Enhanced photosynthetic performance drives limonene production in the L*rpoD* strain. A: Differentially regulated proteins in *Synechococcus* L*rpoD* vs L1118 cells are depicted in the volcano plot. Blue and orange dots represent proteins with their abundances significantly different in these two strains. Gray dots are proteins showing no significant abundance changes in two strains, B: Normalized and averaged full absorbance spectra of cultures from Day 2–5 (individual day measurements are depicted in Fig. S3), and C: Oxygen evolution rates of *Synechococcus* L1118 and L*rpoD*. Cultures were grown continuously under 50 µmol photons $m^{-2}{\cdot}s^{-1}$ light at 30 °C with 20 mM bicarbonate as the substrate for 5 days and all measurements were taken every 24 h. Error bar indicates SD; multiple unpaired Student's t-test was used to compare protein abundances and oxygen evolution rates *, $P < 0.05$; **, $P < 0.01$; ***, $P < 0.001$; and ****, $P < 0.0001$. (For interpretation of the references to colour in this figure legend, the reader is referred to the Web version of this article.)

sensitivity due to the production of reactive oxygen species (ROS) (Abasova et al., 2011). The highly abundant proteins in the L*rpoD* strain include Psb27, Psb28, CP43, CP47, PsbN, and PsbH. These proteins participate in PSII biogenesis, assembly, and proper functioning (Bečková et al., 2017; Dobáková et al., 2009; Komenda et al., 2005, 2012; Torabi et al., 2014). Taken together, the proteomics results suggest enhanced light absorption and photosynthetic efficiency in the L*rpoD* strain. We further measured whole-cell oxygen evolution rates of *Synechococcus* L1118 and L*rpoD* strains grown under 50 μmol photons $m^{-2}{\cdot}s^{-1}$ at 30 °C. As expected, the L*rpoD* cells exhibited consistently higher oxygen evolution rates compared to the L1118 cells (Fig. 2C), in agreement with the proteomics results.

The comparative proteomics further suggests a more robust carbon metabolism in the L*rpoD* strain to leverage the high light energy conversion. Both the large and small subunits of Rubisco (CbbL and CbbS) were found to be significantly more abundant in the L*rpoD* strain (Fig. 2A and S2D). Glyceraldehyde 3-phosphate dehydrogenase (Gap2), the key enzyme in the reduction phase of the Calvin-Benson cycle (Koksharova et al., 1998), was also found to be significantly more abundant in L*rpoD* strain (Fig. 2A), Collectively, the proteomics data is indicative of higher carbon fixation in L*rpoD* strain, resulting in higher photosynthate output that benefits limonene production. Interestingly, the higher photosynthetic rate in the L*rpoD* strain does not seem to be enough to drive more cell divisions as similar growth was observed in L*rpoD* and L1118 cells. The increased carbon fixation in the L*rpoD* strain thus most likely led to more abundant carbon sink molecules such as glycogen or more pigment molecules (Fig. 2B).

3.3. Limonene synthesis serves as a non-native carbon sink for enhanced photosynthesis

The higher limonene production in the L*rpoD* strain suggests that limonene synthesis can serve as a non-native carbon sink for enhanced photosynthesis. However, it is not clear how limonene biosynthesis was able to compete for photosynthates with native carbon sinks such as glycogen and sucrose synthesis. Glycogen is the main storage compound in *S. elongatus* and is essential for cell survival in various stress conditions (Luan et al., 2019; Shinde et al., 2020). A basal level of sucrose is also observed in low salt-tolerant cyanobacteria like *S. elongatus* (Kirsch et al., 2019). To understand whether limonene synthesis can actively compete for photosynthates with native carbon sinks, we first conducted computational modeling to simulate how limonene flux changes with enhanced photosynthate output from the Calvin-Benson cycle. A previously published Genome-Scale Model (GEM) *i*JB785 of *S. elongatus* (Broddrick et al., 2016) was modified by introducing the limonene synthase reaction to generate the new model. Since the GEM cannot reflect regulatory roles such as sigma factor overexpression, we approximated the enhanced photosynthesis by simulating increased light intensity. Specifically, flux balance analysis (FBA) and flux variability analysis (FVA) were performed with the irradiance set to 30 μmol photons $m^{-2}{\cdot}s^{-1}$ and 50 μmol photons $m^{-2}{\cdot}s^{-1}$, respectively. Under the higher light, the obtained optimal solution reveals an increased carbon fixation and higher photosynthate output. Interestingly, the higher photosynthate output (e.g., glyceraldehyde 3-phosphate flux) has led to an increased flux toward both the native carbon sink glycogen synthesis and the non-native sink limonene synthesis, which is reflected by an upward shift of flux boundaries for key reactions in both glycogen synthesis (GLCS3) and limonene synthesis (1-deoxy-D-xylulose 5-phosphate synthase (DXPS) reaction) (Fig. 3A, Fig. S4, and Dataset S1). On the other hand, sucrose synthesis shows no flux in the *in silico* analysis because it is not part of the objective function for growth maximization. The simulation results support the conclusion that limonene synthesis can serve as a non-native carbon sink for enhanced photosynthesis.

To further validate the modeling results, we determined glycogen and sucrose contents in *Synechococcus* L1118 and L*rpoD* strains during their growth. The results showed notable decreases in sucrose content in the *Synechococcus* L*rpoD* strain compared to the *Synechococcus* L1118 (Fig. 3B and S1). On the other hand, glycogen content was significantly

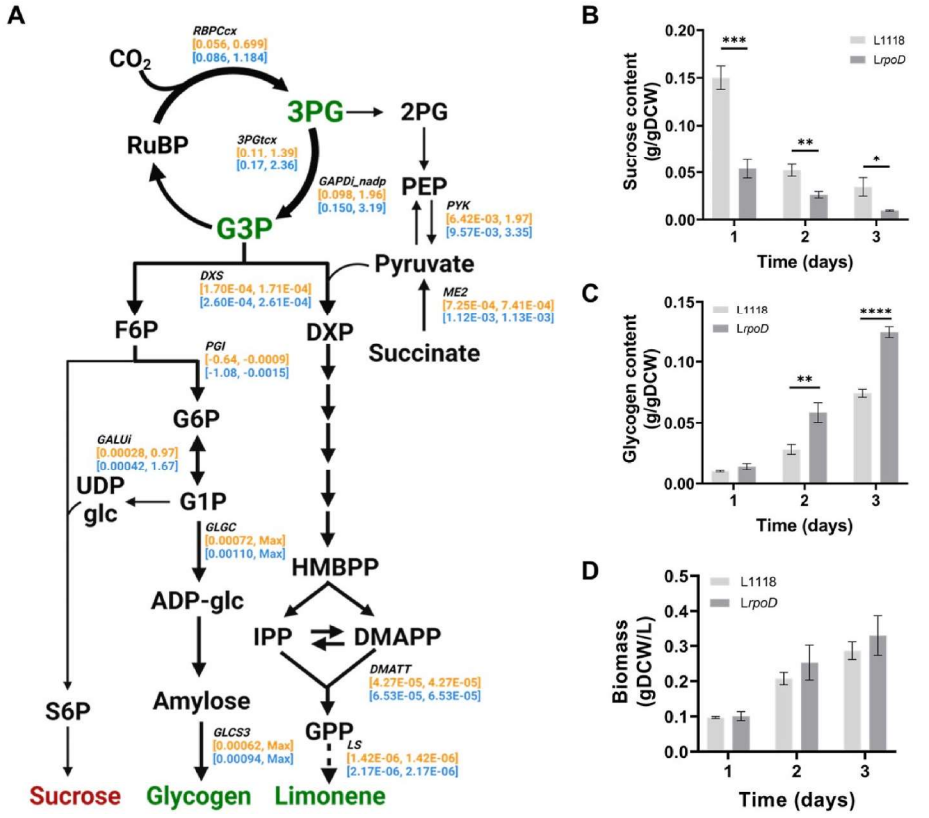

Fig. 3. Native and non-native carbon sinks compete for carbon intermediates in engineered *S. elongatus* strains. A: Carbon flux changes, represented as [minimum flux, maximum flux], along with the specific steps in carbon metabolic pathways. Relevant steps are labeled by the enzyme name, flux values (mmol·$gDW^{-1}{\cdot}h^{-1}$) at 30 μmol photons $m^{-2}{\cdot}s^{-1}$ (orange) and 50 μmol photons $m^{-2}{\cdot}s^{-1}$ (blue). B: Sucrose content, and C: Glycogen content in *Synechococcus* L*rpoD* cells compared to *Synechococcus* L1118. Cultures were grown continuously under 50 μmol photons $m^{-2}{\cdot}s^{-1}$ light at 30 °C for 5 days and all measurements were taken every 24 h. Error bar indicates SD; multiple unpaired Student's t-test was used to compare the carbohydrate levels *, $P < 0.05$; **, $P < 0.01$; ***, $P < 0.001$; and ****, $P < 0.0001$. (For interpretation of the references to colour in this figure legend, the reader is referred to the Web version of this article.)

higher in the *Synechococcus* L*rpoD* strain, resulting in an approximately 15% increase in biomass at the end of 3 days (Fig. 3C and D). In addition, the proteomics results also support the carbon flux diversion toward glycogen rather than other cell metabolites. Phosphoglycerate mutase (Pgm), the enzyme in the lower part of glycolysis to convert 3-phosphoglycerate (3PGA) to 2-phosphoglycerate (2PGA), is a key flux-controlling enzyme in cyanobacteria to divert carbon flux toward either glycogen or pyruvate. A recent study in *Synechocystis* sp. PCC 6803 showed that under nitrogen deprivation, a newly annotated protein PirC inhibits the enzyme activity of Pgm, restricting carbon flux toward pyruvate and leading to the accumulation of glycogen (Orthwein et al., 2021). Our proteomics results show that Pgm1 and pyruvate kinase were both significantly decreased in L*rpoD* cells (Fig. 2A and S2D), suggesting a lower flux toward pyruvate. In the meantime, several enzymes downstream of pyruvate metabolism including those in the lipid biosynthesis and TCA pathway were also significantly decreased in L*rpoD* cells. Specifically, abundances of acetyl-CoA carboxylase complex subunits (AccA, AccC, and AccD) were significantly decreased, suggesting a lower flux toward lipid biosynthesis (Fig. S2D). Fumarase (Synpcc7942_1007) and malic enzyme (Synpcc7942_1297) in the TCA pathway also showed significantly lower levels in the *Synechococcus* L*rpoD* than the L1118 strain (Fig. S2D). The proteomics results support the observed glycogen accumulation by restricting carbon flux toward the lower part of glycolysis. Concomitantly, α-1,4-glucan phosphorylase (GlgP), the enzyme involved in glycogen degradation, had significantly decreased levels in *Synechococcus* L*rpoD* cells (Fig. S2D) suggesting down-regulation of glycogen mobilization. Sucrose-phosphate synthase, a key enzyme for sucrose synthesis, was also significantly lower in *Synechococcus* L*rpoD* cells. These results show that glycogen accumulation serves as a major outlet for enhanced photosynthesis.

In the meantime, the abundance of IspG, a key enzyme in the MEP pathway, was found to be significantly lower in the *Synechococcus* L*rpoD* strain compared to *Synechococcus* L1118 (Fig. 2A), which suggests a lower flux toward the MEP-derived limonene biosynthesis. The increased limonene production in the L*rpoD* cells in comparison to L1118 seems to contradict the enzyme expression necessary for pyruvate generation through glycolysis. It is thus likely that pyruvate is generated through an alternative route to serve as one of the starting substrates for the MEP pathway. Carbon flux is determined by both enzyme kinetics and thermodynamics. Enhanced photosynthesis leads to a higher output of the photosynthate G3P, the key substrate for the MEP-derived terpene biosynthesis. The higher limonene titer in *Synechococcus* L*rpoD* cells suggests that thermodynamics has a stronger impact on terpene flux. Previous research in *E. coli* showed that increased G3P rather than pyruvate concentration could drive a higher terpene flux, presumably due to the decarboxylating mechanism of the 1-deoxy-D-xylulose-5-phosphate synthase, DXS (Farmer and Liao, 2001). Another study also tested the influence of thermodynamics on carbon flux in yeast, in which they show that enhancing substrate concentrations has a much stronger impact than enzymes on pathway flux (Hackett et al., 2016). We argue that for low-flux pathways such as terpene biosynthesis, the thermodynamic effect has a much stronger impact in enhancing pathway flux due to the inherent low enzyme activities in the terpene pathways (Bar-Even et al., 2011).

3.4. Enhancing terpene flux requires a strong thermodynamic driving force

Enhancing photosynthesis through sigma factor overexpression can lead to higher limonene production, suggesting a strong impact of "source" improvement in supporting high terpene production in cyanobacteria. Compared to terrestrial plants, CO_2 delivery in aquatic photosynthetic organisms such as cyanobacteria is further limited by low CO_2 solubility in water. To bypass this limitation, cyanobacteria evolved a carbon concentrating mechanism (CCM) to accumulate bicarbonate in the cytosol via bicarbonate transporters and convert it into CO_2 in carboxysomes to spatially enrich the environment harboring Rubisco with CO_2 (Nishimura et al., 2008; Price et al., 2008).

To validate our thermodynamics hypothesis, we sought to explore the efficacy of enhancing limonene production by increasing CO_2 availability in cells. Overexpressing BicA, a low-affinity high flux bicarbonate transporter has been associated with enhanced biomass (Kamennaya et al., 2015), increased growth rate, and higher accumulation of glycogen (Gupta et al., 2020). We thus overexpressed the *bicA* gene from *Synechocystis* sp. PCC 6803 in the *Synechococcus* L1118 strain and monitored limonene production. Our data indicate higher limonene productivity in *Synechococcus* L*bicA* strain compared to *Synechococcus* L1118 (Fig. 4A) with no significant growth alteration (Fig. 4B), supporting our hypothesis that enhanced "source" capacity could lead to higher limonene titer, also exhibited by higher specific productivity in L*bicA* strains (Fig.S5A). It is worth mentioning that the productivity increase of L*bicA* was not as high when compared to *Synechococcus* L*rpoD* strain, presumably due to the strong flux competition by the native carbon sink glycogen, evidenced by a significant increase of glycogen rather than sucrose in the L*bicA* strain (Fig. 4C and D).

The CO_2 gas could directly diffuse into cells without using the energy-consuming bicarbonate pump in the cell membrane. We thus tested limonene production with 5% CO_2 at elevated light and temperature conditions to leverage a high photosynthetic efficiency for robust CO_2 fixation. Under the optimal growth condition, *Synechococcus* L*rpoD* cells showed significantly higher limonene productivity in comparison to L1118 (Fig. 4E and S5B), whereas their growth was comparable, and considerably faster in comparison to the growth under standard conditions (Fig. 4F). At the end of 7 days, L*rpoD* accumulated limonene to a titer of about 19 mg/L with a maximum productivity of 4.3 mg/L/day on day 5 (Fig. 4G).

Collectively, terpene production is both "source" (substrate availability) and "sink" (terpene synthesis capacity) limited. The source limitation cannot be overcome solely by strengthening the terpene sink due to slow enzyme kinetics in the terpene synthesis pathway (weak "pull" capacity). In heterotrophic terpene engineering, when substrate (carbohydrate) is not limited, a relatively high terpene flux is attainable by further improving enzyme kinetics in the terpene synthesis pathway. However, the source limitation in cyanobacteria is hard to overcome due to the low photosynthetic efficiency for CO_2 fixation. This could explain why cyanobacterial terpene engineering focusing on kinetics improvement has not been successful in the field. Our results show that improving bicarbonate transport (*Synechococcus* L*bicA*) or using high percentage CO_2 to increase overall substrate availability (strong "push" effect) could improve the source limitation and enhance limonene production in cyanobacteria.

4. Conclusion

Engineering cyanobacteria holds great promise for carbon-neutral terpenoid production in an emerging bioeconomy. However, the field has been troubled by the low productivity associated with photosynthetic terpenoid production. In this study, engineering sigma factors in *S. elongatus* led to enhanced photosynthetic efficiency as evidenced by higher light reaction efficiency and increased biomass in the engineered strain. The increased photosynthate output was shared by both the native glycogen carbon sink and the non-native carbon sink limonene biosynthesis. Although enzyme levels in the MEP pathway were lowered in the engineered strain, a significant improvement in limonene production was achieved in *S. elongatus*, most likely through increased substrate input to the MEP pathway supported by increased light reaction efficiency. We conclude that enhancing the productivity of low-flux pathways such as terpenoid biosynthesis requires a strong "push" effect determined by thermodynamics. With a strong "source" capacity, improving pathway enzyme kinetics could lead to further improvement of pathway carbon flux. This conclusion corroborates with the finding that high limonene productivity (8.2 mg/L/day) could be achieved in

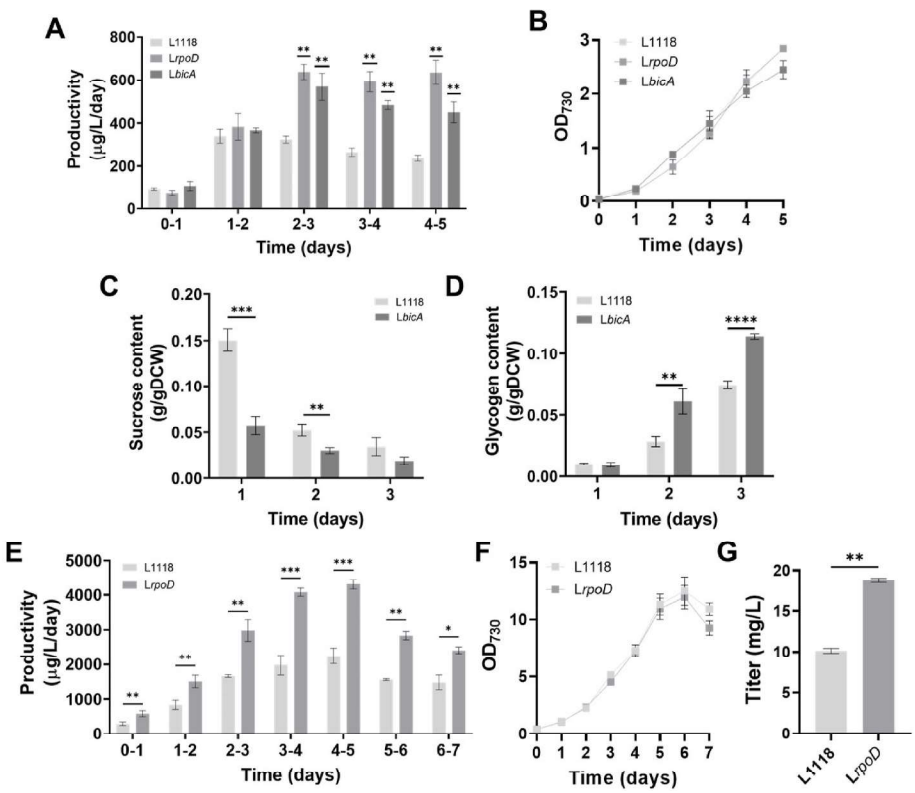

Fig. 4. Increased carbon substrate uptake enhances limonene production in *S. elongatus* strains. Limonene productivity (A) and growth profile (B) of *Synechococcus* L1118, L*rpoD,* and L*bicA*. Sucrose content (C) and glycogen content (D) of L1118 and L*bicA* grown under continuous 50 μmol photons $m^{-2}{\cdot}s^{-1}$ light at 30 °C with 20 mM bicarbonate as a substrate for 7 days. All measurements were taken every 24 h. The sucrose and glycogen content of *Synechococcus* L1118 is the same as Fig. 3 B–C. Limonene productivity (E), growth (F), and limonene titer (G) of *Synechococcus* L1118 and L*rpoD* when grown under optimized growth conditions (CD medium aerated with 5% CO_2 at varying light intensities and 37 °C). Error bar indicates SD; unpaired Student's t-test was used to compare limonene productivity and titer *, $P < 0.05$; **, $P < 0.01$; ***, $P < 0.001$; and ****, $P < 0.0001$.

the fast-growing cyanobacterium *S. elongatus* UTEX 2973 with high photosynthetic efficiency (Lin et al., 2021). In addition, a more recent study utilized a low-volume high-cell-density cultivation system to leverage high light to enhance photosynthetic efficiency in *Synechocystis* sp. PCC 6803, achieving 180 mg/L bisabolene titer after a 10-day growth (Rodrigues and Lindberg, 2021). In heterotrophic terpenoid engineering, an overall high substrate amount, normally attained through the fed-batch experiment, is required to attain high titers of end terpenoid products. In photosynthetic terpenoid production, leveraging high photosynthetic efficiency to enhance overall carbon substrate input thus resembles the high substrate input in heterotrophs, representing a promising strategy to reach high titer of terpenoids in metabolic engineering efforts.

Author contributions

Shrameeta Shinde: Methodology, Investigation, Visualization, Writing- Original Draft; Sonali Singapuri: Methodology, Investigation; Zhenxiong Jiang: Methodology, Software, Visualization, Writing – Review & Editing; Bin Long: Investigation, Validation; Danielle Wilcox: Investigation; Camille Klatt: Investigation; J. Andrew Jones: Resources, Writing - Reviewing & Editing; Joshua S. Yuan: Resources, Funding acquisition; Xin Wang: Conceptualization, Methodology, Formal Analysis, Resources, Supervision, Project administration, Funding acquisition, Writing - Reviewing & Editing.

Declaration of competing interest

The authors declare that they have no known competing financial interests or personal relationships that could have appeared to influence the work reported in this paper.

Acknowledgment

We would like to thank Xiaohui Zhang for constructing the *Synechococcus* L*bicA* strain used in this study. We also thank Andor Kiss and Xiaoyun Deng of the Center for Bioinformatics and Functional Genomics at Miami University for providing access to various instruments used for data collection in this study. We thank Rachael Morgan-Kiss for providing access to the Multi-Cultivator MC 1000-OD. This work was supported by the start-up fund to X.W. from Miami University and partially supported by the National Science Foundation grant number 2042182. J.A.J. would like to acknowledge start-up funding from the College of Engineering and Computing at Miami University. J.S.Y. would like to thank Dr. John Hood's generous donation of Hood Fund for Sustainability.

Appendix A. Supplementary data

Supplementary data to this article can be found online at https://doi.org/10.1016/j.mec.2022.e00193.

References

Abasova, L., Deák, Z., Schwarz, R., Vass, I., 2011. The role of the PsbU subunit in the light sensitivity of PSII in the cyanobacterium *Synechococcus* 7942. J. Photochem. Photobiol. B Biol. 105, 149–156. https://doi.org/10.1016/J.JPHOTOBIOL.2011.08.004.

Ajikumar, P.K., Tyo, K., Carlsen, S., Mucha, O., Phon, T.H., Stephanopoulos, G., 2008. Terpenoids: opportunities for biosynthesis of natural product drugs using engineered microorganisms. Mol. Pharm. 5, 167–190. https://doi.org/10.1021/mp700151b.

Balint, I., Bhattacharya, J., Perelman, A., Schatz, D., Moskovitz, Y., Keren, N., Schwarz, R., 2006. Inactivation of the extrinsic subunit of photosystem II, PsbU, in *Synechococcus* PCC 7942 results in elevated resistance to oxidative stress. FEBS Lett. 580, 2117–2122. https://doi.org/10.1016/J.FEBSLET.2006.03.020.

Bar-Even, A., Noor, E., Savir, Y., Liebermeister, W., Davidi, D., Tawfik, D.S., Milo, R., 2011. The moderately efficient enzyme: evolutionary and physicochemical trends shaping enzyme parameters. Biochemistry 50, 4402–4410. https://doi.org/10.1021/bi2002289.

Bečková, M., Gardian, Z., Yu, J., Konik, P., Nixon, P.J., Komenda, J., 2017. Association of Psb28 and Psb27 proteins with PSII-PSI supercomplexes upon exposure of *Synechocystis* sp. PCC 6803 to High Light. Mol. Plant 10, 62–72. https://doi.org/10.1016/J.MOLP.2016.08.001.

Bersanini, L., Battchikova, N., Jokel, M., Rehman, A., Vass, I., Allahverdiyeva, Y., Aro, E.-M., 2014. Flavodiiron protein flv2/flv4-related photoprotective mechanism

dissipates excitation pressure of PSII in cooperation with phycobilisomes in cyanobacteria. Plant Physiol. 164 (805) https://doi.org/10.1104/PP.113.231969.
Broddrick, J.T., Rubin, B.E., Welkie, D.G., Du, N., Mih, N., Diamond, S., Lee, J.J., Golden, S.S., Palsson, B.O., 2016. Unique attributes of cyanobacterial metabolism revealed by improved genome-scale metabolic modeling and essential gene analysis. Proc. Natl. Acad. Sci. U. S. A 113, E8344–E8353. https://doi.org/10.1073/PNAS.1613446113.
Carvalho, P.C., Lima, D.B., Leprevost, F.V., Santos, M.D.M., Fischer, J.S.G., Aquino, P.F., Moresco, J.J., Yates, J.R., Barbosa, V.C., 2016. Integrated analysis of shotgun proteomic data with PatternLab for proteomics 4.0. Nat. Protoc. 11, 102–117. https://doi.org/10.1038/nprot.2015.133.
Choi, S.Y., Park, B., Choi, I., Sim, S.J., Lee, S., 2016. Transcriptome landscape of *Synechococcus elongatus* PCC 7942 for nitrogen starvation responses using RNA-seq. Nat. Publ. Gr 1–10. https://doi.org/10.1038/srep30584.
Chuck, C.J., Donnelly, J., 2014. The compatibility of potential bioderived fuels with Jet A-1 aviation kerosene. Appl. Energy 118, 83–91. https://doi.org/10.1016/j.apenergy.2013.12.019.
Davies, F.K., Work, V.H., Beliaev, A.S., Posewitz, M.C., 2014. Engineering limonene and bisabolene production in wild type and a glycogen-deficient mutant of *Synechococcus* sp. PCC 7002. Front. Bioeng. Biotechnol. 2 (21) https://doi.org/10.3389/fbioe.2014.00021.
De Porcellinis, A., Frigaard, N.U., Sakuragi, Y., 2017. Determination of the glycogen content in cyanobacteria. JoVE. https://doi.org/10.3791/56068 e56068.
Dobáková, M., Sobotka, R., Tichý, M., Komenda, J., 2009. Psb28 protein is involved in the biogenesis of the photosystem II inner antenna CP47 (PsbB) in the cyanobacterium *Synechocystis* sp. PCC 6803. Plant Physiol. 149, 1076–1086. https://doi.org/10.1104/PP.108.130039.
Englund, E., Andersen-Ranberg, J., Miao, R., Hamberger, B., Lindberg, P., 2015. Metabolic engineering of *Synechocystis* sp. PCC 6803 for production of the plant diterpenoid manoyl oxide. ACS Synth. Biol. 4, 1270–1278. https://doi.org/10.1021/acssynbio.5b00070.
Englund, E., Pattanaik, B., Ubhayasekera, S., Stensjö, K., Bergquist, J., 2014. Production of squalene in *Synechocystis* sp. PCC 6803. PLoS One 9, e90270. https://doi.org/10.1371/journal.pone.0090270.
Farmer, W.R., Liao, J.C., 2001. Precursor balancing for metabolic engineering of lycopene production in *Escherichia coli*. Biotechnol. Prog. 17, 57–61. https://doi.org/10.1021/BP000137T.
Fleming, K.E., O'Shea, E.K., 2018. An RpaA-dependent sigma factor cascade sets the timing of circadian transcriptional rhythms in *Synechococcus elongatus* cell reports an RpaA-dependent sigma factor cascade sets the timing of circadian transcriptional rhythms in Synechococcus elongatus. Cell Rep. 25, 2937–2945. https://doi.org/10.1016/j.celrep.2018.11.049.
Formighieri, C., Melis, A., 2016. Sustainable heterologous production of terpene hydrocarbons in cyanobacteria. Photosynth. Res. 130, 123–135. https://doi.org/10.1007/s11120-016-0233-2.
Formighieri, C., Melis, A., 2014. Regulation of β-phellandrene synthase gene expression, recombinant protein accumulation, and monoterpene hydrocarbons production in *Synechocystis* transformants. Planta 240, 309–324. https://doi.org/10.1007/s00425-014-2080-8.
Gao, X., Gao, F., Liu, D., Zhang, H., Nie, X., Yang, C., 2016. Environmental Science Engineering the methylerythritol phosphate pathway in cyanobacteria for photosynthetic. Energy Environ. Sci. 9, 1400–1411. https://doi.org/10.1039/C5EE03102H.
Golden, S.S., Brusslan, J., Haselkorn, R., 1987. Genetic engineering of the cyanobacterial chromosome. Methods Enzymol. 153, 215–231. https://doi.org/10.1016/0076-6879(87)53055-5.
Gupta, J.K., Rai, P., Jain, K.K., Srivastava, S., 2020. Overexpression of bicarbonate transporters in the marine cyanobacterium *Synechococcus* sp. PCC 7002 increases growth rate and glycogen accumulation. Biotechnol. Biofuels 13 (17). https://doi.org/10.1186/s13068-020-1656-8.
Hackett, S.R., Zanotelli, V.R.T., Xu, W., Goya, J., Park, J.O., Perlman, D.H., Gibney, P.A., Botstein, D., Storey, J.D., Rabinowitz, J.D., 2016. Systems-level analysis of mechanisms regulating yeast metabolic flux (80). Science 354. https://doi.org/10.1126/science.aaf2786, 2786–15.
Hakkila, K., Antal, T., Gunnelius, L., Kurkela, J., Matthijs, H.C.P., Tyystjärvi, E., Tyystjärvi, T., 2013. Group 2 sigma factor mutant ΔsigCDE of the cyanobacterium *Synechocystis* sp. PCC 6803 Reveals Functionality of Both Carotenoids and Flavodiiron Proteins in Photoprotection of Photosystem II. Plant Cell Physiol 54, 1780–1790. https://doi.org/10.1093/PCP/PCT123.
Halfmann, C., Gu, L., Zhou, R., 2014. Engineering cyanobacteria for the production of a cyclic hydrocarbon fuel from CO2 and H2O. Green Chem. 16, 3175–3185.
Huckauf, J., Nomura, C., Forchhammer, K., Hagemann, M., 2000. Stress responses of *Synechocystis* sp. strain PCC 6803 mutants impaired in genes encoding putative alternative sigma factors. Microbiology 146, 2877–2889. https://doi.org/10.1099/00221287-146-11-2877.
Imamura, S., Yoshihara, S., Nakano, S., Shiozaki, N., Yamada, A., Tanaka, K., Takahashi, H., Asayama, M., Shirai, M., 2003. Purification, characterization, and gene expression of all sigma factors of RNA polymerase in a cyanobacterium. J. Mol. Biol. 325, 857–872. https://doi.org/10.1016/S0022-2836(02)01242-1.
Kaczmarzyk, D., Anfelt, J., Särnegrim, A., Hudson, E.P., 2014. Overexpression of sigma factor SigB improves temperature and butanol tolerance of *Synechocystis* sp. PCC6803. J. Biotechnol. 182–183, 54–60. https://doi.org/10.1016/j.jbiotec.2014.04.017.
Kamennaya, N.A., Ahn, S.E., Park, H., Bartal, R., Sasaki, K.A., Holman, H.Y., Jansson, C., 2015. Installing extra bicarbonate transporters in the cyanobacterium *Synechocystis* sp. PCC6803 enhances biomass production. Metab. Eng. 29, 76–85. https://doi.org/10.1016/j.ymben.2015.03.002.
Kanesaki, Y., Suzuki, I., Allakhverdiev, S.I., Mikami, K., Murata, N., 2002. Salt stress and hyperosmotic stress regulate the expression of different sets of genes in *Synechocystis* sp. PCC 6803. Biochem. Biophys. Res. Commun. 290, 339–348. https://doi.org/10.1006/BBRC.2001.6201.
Kirsch, F., Klähn, S., Hagemann, M., 2019. Salt-regulated accumulation of the compatible solutes sucrose and glucosylglycerol in cyanobacteria and its biotechnological potential. Front. Microbiol. https://doi.org/10.3389/fmicb.2019.02139.
Kiyota, H., Okuda, Y., Ito, M., Hirai, M.Y., Ikeuchi, M., 2014. Engineering of cyanobacteria for the photosynthetic production of limonene from CO_2. J. Biotechnol. 185, 1–7. https://doi.org/10.1016/j.jbiotec.2014.05.025.
Knoot, C.J., Ungerer, J., Wangikar, P.P., Pakrasi, H.B., 2018. Cyanobacteria: promising biocatalysts for sustainable chemical production. J. Biol. Chem. https://doi.org/10.1074/jbc.R117.815886.
Koksharova, O., Schubert, M., Shestakov, S., Cerff, R., 1998. Genetic and biochemical evidence for distinct key functions of two highly divergent GAPDH genes in catabolic and anabolic carbon flow of the cyanobacterium *Synechocystis* sp. PCC 6803. Plant Mol. Biol. 36, 183–194.
Komenda, J., Knoppová, J., Kopečná, J., Sobotka, R., Halada, P., Yu, J., Nickelsen, J., Boehm, M., Nixon, P.J., 2012. The Psb27 assembly factor binds to the CP43 complex of photosystem II in the cyanobacterium *Synechocystis* sp. PCC 6803. Plant Physiol. 158, 476–486. https://doi.org/10.1104/PP.111.184184.
Komenda, J., Tichý, M., Eichacker, L.A., 2005. The PsbH protein is associated with the inner antenna CP47 and facilitates D1 processing and incorporation into PSII in the cyanobacterium *Synechocystis* PCC 6803. Plant Cell Physiol. 46, 1477–1483. https://doi.org/10.1093/PCP/PCI159.
Lin, P.-C., Zhang, F., Pakrasi, H.B., 2021. Enhanced limonene production in a fast-growing cyanobacterium through combinatorial metabolic engineering. Metab. Eng. Commun. https://doi.org/10.1016/j.mec.2021.e00164 e00164.
Lin, P.C., Pakrasi, H.B., 2019. Engineering cyanobacteria for production of terpenoids. Planta 249, 145–154. https://doi.org/10.1007/s00425-018-3047-y.
Lin, P.C., Saha, R., Zhang, F., Pakrasi, H.B., 2017. Metabolic engineering of the pentose phosphate pathway for enhanced limonene production in the cyanobacterium *Synechocystis* sp. PCC. Sci. Rep. 7 (17503) https://doi.org/10.1038/s41598-017-17831-y.
Lindberg, P., Park, S., Melis, A., 2010. Engineering a platform for photosynthetic isoprene production in cyanobacteria, using *Synechocystis* as the model organism. Metab. Eng. 12, 70–79. https://doi.org/10.1016/j.ymben.2009.10.001.
Luan, G., Zhang, S., Wang, M., Lu, X., 2019. Progress and perspective on cyanobacterial glycogen metabolism engineering. Biotechnol. Adv. 37, 771–786. https://doi.org/10.1016/j.biotechadv.2019.04.005.
Martins, B.M., Das, A.K., Antunes, L., Locke, J.C., 2016. Frequency doubling in the cyanobacterial circadian clock. Mol. Syst. Biol. 12, 896. https://doi.org/10.15252/MSB.20167087.
Masojídek, J., Torzillo, G., Koblížek, M., 2013. Photosynthesis in microalgae. In: Handbook of Microalgal Culture: Applied Phycology and Biotechnology, second ed. John Wiley & Sons, Ltd, pp. 21–36. https://doi.org/10.1002/9781118567166.CH2.
Melis, A., 2013. Carbon partitioning in photosynthesis. Curr. Opin. Chem. Biol. https://doi.org/10.1016/j.cbpa.2013.03.010.
Nishimura, T., Takahashi, Y., Yamaguchi, O., Suzuki, H., Maeda, S., Omata, T., 2008. Mechanism of low CO_2-induced activation of the cmp bicarbonate transporter operon by a LysR family protein in the cyanobacterium *Synechococcus elongatus* strain PCC 7942. Mol. Microbiol. 68, 98–109. https://doi.org/10.1111/J.1365-2958.2008.06137.X.
Noor, E., Bar-Even, A., Flamholz, A., Reznik, E., Liebermeister, W., Milo, R., 2014. Pathway thermodynamics highlights kinetic obstacles in central metabolism. PLoS Comput. Biol. 10, e1003483. https://doi.org/10.1371/JOURNAL.PCBI.1003483.
Noor, E., Flamholz, A., Bar-Even, A., Davidi, D., Milo, R., Liebermeister, W., 2016. The protein cost of metabolic fluxes: prediction from enzymatic rate laws and cost minimization. PLoS Comput. Biol. 12, e1005167. https://doi.org/10.1371/JOURNAL.PCBI.1005167.
Orthwein, T., Scholl, J., Spät, P., Lucius, S., Koch, M., Macek, B., Hagemann, M., Forchhammer, K., 2021. The novel PII-interactor PirC identifies phosphoglycerate mutase as key control point of carbon storage metabolism in cyanobacteria. Proc. Natl. Acad. Sci. Unit. States Am. 118 https://doi.org/10.1073/PNAS.2019988118 e2019988118.
Osanai, T., Numata, K., Oikawa, A., Kuwahara, A., Iijima, H., Doi, Y., Tanaka, K., Saito, K., Yokota Hirai, M., 2013. Increased bioplastic production with an RNA polymerase sigma factor SigE during nitrogen starvation in *Synechocystis* sp. PCC 6803. DNA Res. 20, 525–535. https://doi.org/10.1093/dnares/dst028.
Perez-Riverol, Y., Csordas, A., Bai, J., Bernal-Llinares, M., Hewapathirana, S., Kundu, D. J., Inuganti, A., Griss, J., Mayer, G., Eisenacher, M., Pérez, E., Uszkoreit, J., Pfeuffer, J., Sachsenberg, T., Yılmaz, Ş., Tiwary, S., Cox, J., Audain, E., Walzer, M., Jarnuczak, A.F., Ternent, T., Brazma, A., Vizcaíno, J.A., 2019. The PRIDE database and related tools and resources in 2019: improving support for quantification data. Nucleic Acids Res. 47, D442–D450. https://doi.org/10.1093/NAR/GKY1106.
Price, G.D., Badger, M.R., Woodger, F.J., Long, B.M., 2008. Advances in understanding the cyanobacterial CO_2-concentrating-mechanism (CCM): functional components, Ci transporters, diversity, genetic regulation and prospects for engineering into plants. J. Exp. Bot. 59, 1441–1461. https://doi.org/10.1093/JXB/ERM112.
Rodrigues, J.S., Lindberg, P., 2021. Metabolic engineering of *Synechocystis* sp. PCC 6803 for improved bisabolene production. Metab. Eng. Commun 12, e00159. https://doi.org/10.1016/J.MEC.2020.E00159.
Rubin, B.E., Wetmore, K.M., Price, M.N., Diamond, S., Shultzaberger, R.K., Lowe, L.C., Curtin, G., Arkin, A.P., Deutschbauer, A., Golden, S.S., 2015. The essential gene set

of a photosynthetic organism. Proc. Natl. Acad. Sci. Unit. States Am. 112, E6634–E6643. https://doi.org/10.1073/PNAS.1519220112.

Shen, J.R., Ikeuchi, M., Inoue, Y., 1997. Analysis of the psbU gene encoding the 12-kDa extrinsic protein of photosystem II and studies on its role by deletion mutagenesis in *Synechocystis* sp. PCC 6803. J. Biol. Chem. 272, 17821–17826. https://doi.org/10.1074/JBC.272.28.17821.

Shinde, S., Zhang, X., Singapuri, S.P., Kalra, I., Liu, X., Morgan-Kiss, R.M., Wang, X., 2020. Glycogen metabolism supports photosynthesis start through the oxidative pentose phosphate pathway in cyanobacteria. Plant Physiol. 182, 507–517. https://doi.org/10.1104/pp.19.01184.

Srivastava, A., Varshney, R.K., Shukla, P., 2021. Sigma factor modulation for cyanobacterial metabolic engineering. Trends Microbiol. 29, 266–277. https://doi.org/10.1016/j.tim.2020.10.012.

Torabi, S., Umate, P., Manavski, N., Plöchinger, M., Kleinknecht, L., Bogireddi, H., Herrmann, R.G., Wanner, G., Schröder, W.P., Meurer, J., 2014. PsbN is required for assembly of the photosystem II reaction center in *Nicotiana tabacum*. Plant Cell 26 (1183). https://doi.org/10.1105/TPC.113.120444.

Tuominen, I., Tyystjärvi, E., Tyystjärvi, T., 2003. Expression of primary sigma factor (PSF) and PSF-like sigma factors in the cyanobacterium *Synechocystis* sp. strain PCC 6803. J. Bacteriol. 185, 1116–1119. https://doi.org/10.1128/JB.185.3.1116-1119.2003.

Veerman, J., Bentley, F., Eaton-Rye, J., Mullineaux, C., Vasil'ev, S., Bruce, D., 2005. The PsbU subunit of photosystem II stabilizes energy transfer and primary photochemistry in the Phycobilisome−Photosystem II assembly of *Synechocystis* sp. PCC 6803. Biochemistry 44, 16939–16948. https://doi.org/10.1021/BI051137A.

Wang, X., Liu, W., Xin, C., Zheng, Y., Cheng, Y., Sun, S., Li, R., Zhu, X., 2016. Enhanced limonene production in cyanobacteria reveals photosynthesis limitations 113, 14225–14230. https://doi.org/10.1073/pnas.1613340113.

Wang, X., Ort, D.R., Yuan, J.S., 2015. Photosynthetic terpene hydrocarbon production for fuels and chemicals. Plant Biotechnol. J. 13, 137–146. https://doi.org/10.1111/pbi.12343.

Wu, C., Jiang, H., Kalra, I., Wang, X., Cano, M., Maness, P.C., Yu, J., Xiong, W., 2020. A generalized computational framework to streamline thermodynamics and kinetics analysis of metabolic pathways. Metab. Eng. 57, 140–150. https://doi.org/10.1016/J.YMBEN.2019.08.006.

Yoshimura, T., Imamura, S., Tanaka, K., Shirai, M., Asayama, M., 2007. Cooperation of group 2 σ factors, SigD and SigE for light-induced transcription in the cyanobacterium *Synechocystis* sp. PCC 6803. FEBS Lett. 581, 1495–1500. https://doi.org/10.1016/J.FEBSLET.2007.03.010.

Zavřel, T., Sinetova, M.A., Červený, J., 2015. Measurement of chlorophyll a and carotenoids concentration in cyanobacteria. Bio-protocol 5, e1467.

Zhao, C., Höppner, A., Xu, Q.Z., Gärtner, W., Scheer, H., Zhou, M., Zhao, K.H., 2017. Structures and enzymatic mechanisms of phycobiliprotein lyases CpcE/F and PecE/F. Proc. Natl. Acad. Sci. U. S. A 114, 13170–13175. https://doi.org/10.1073/pnas.1715495114.

Zybailov, B., Mosley, A.L., Sardiu, M.E., Coleman, M.K., Florens, L., Washburn, M.P., 2006. Statistical analysis of membrane proteome expression changes in *Saccharomyces cerevisiae*. J. Proteome Res. 5, 2339–2347. https://doi.org/10.1021/pr060161n.